AMERICAN SOCIETY FOR MICROBIOLOGY | Journal of Virology

Equine Rhinitis A Virus Mutants with Altered Acid Resistance Unveil a Key Role of VP3 and Intrasubunit Interactions in the Control of the pH Stability of the *Aphthovirus* Capsid

Flavia Caridi, Rodrigo Cañas-Arranz, Angela Vázquez-Calvo,* Francisco Sobrino, Miguel A. Martín-Acebes*

Department of Virology and Microbiology, Centro de Biología Molecular Severo Ochoa (CSIC-UAM), Madrid, Spain

ABSTRACT

Equine rhinitis A virus (ERAV) is a picornavirus associated with respiratory disease in horses and is genetically closely related to foot-and-mouth disease virus (FMDV), the prototype aphthovirus. ERAV has recently gained interest as an FMDV alternative for the study of aphthovirus biology, including cell entry and uncoating or antiviral testing. As described for FMDV, current data support that acidic pH inside cellular endosomes triggers ERAV uncoating. In order to provide further insights into aphthovirus uncoating mechanism, we have isolated a panel of ERAV mutants with altered acid sensitivity and that differed on their degree of sensitivity to the inhibition of endosome acidification. These results provide functional evidence of the involvement of acidic pH on ERAV uncoating within endosomes. Remarkably, all amino acid substitutions found in acid-labile or acid-resistant ERAVs were located in the capsid protein VP3, indicating that this protein plays a pivotal role for the control of pH stability of the ERAV capsid. Moreover, all amino acid substitutions mapped at the intraprotomer interface between VP3 and VP2 or between VP3 and the N terminus of VP1. These results expand our knowledge on the regions that regulate the acid stability of aphthovirus capsid and should be taken into account when using ERAV as a surrogate of FMDV.

IMPORTANCE

The viral capsid constitutes a sort of dynamic nanomachine that protects the viral genome against environmental assaults while accomplishing important functions such as receptor attachment for viral entry or genome release. We have explored the molecular determinants of aphthovirus capsid stability by isolating and characterizing a panel of equine rhinitis A virus mutants that differed on their acid sensitivity. All the mutations were located within a specific region of the capsid, the intraprotomer interface among capsid proteins, thus providing new insights into the regions that control the acid stability of aphthovirus capsid. These findings could positively contribute to the development of antiviral approaches targeting aphthovirus uncoating or the refinement of vaccine strategies based on capsid stabilization.

Equine rhinitis A virus (ERAV) is a picornavirus associated with febrile respiratory disease in horses (1, 2). Due to its physical properties and its identification as a respiratory pathogen, ERAV was historically classified into the genus *Rhinovirus* (former Equine rhinovirus-1) of the family *Picornaviridae* (1). However, because of its resemblance at the nucleotide sequence level and at the genomic structure to foot-and-mouth disease virus (FMDV), ERAV has been reclassified into the *Aphthovirus* genus (3). Consistently, ERAV is now considered the phylogenetically most closely related virus to FMDV, which actually constitutes the prototype aphthovirus (http://www.ictvonline.org/virusTaxonomy.asp). Since FMDV is an extremely contagious and pathogenic aphthovirus that can only be manipulated in high-containment biosafety level 3 facilities, the utilization of ERAV as a surrogate for FMDV research has increased in recent years. In this way, ERAV is gaining interest as a suitable model to study aphthovirus cell entry and uncoating or antiviral testing (4–6). Apart from its potential as an alternative tool for FMDV research, the plasticity of its capsid has made of ERAV an interesting model virus for analyzing the structural rearrangements of picornavirus capsids (4, 7).

The ERAV genome consists of a positive-sense, single-stranded RNA molecule about 7.6 kb in length (3). This RNA molecule is enclosed within an ~300-Å diameter nonenveloped icosahedral capsid (4). ERAV capsid is built out of 60 copies of each of the four structural proteins (VP1 to VP4) arranged into 12 pentameric subunits. This capsid is assembled in a stepwise process: five protomer subunits (each made of one copy of each VP) form a stable pentameric intermediate, and 12 pentameric subunits associate to form the capsid (8). Remarkably, ERAV capsid shares with FMDV important physicochemical properties such as its buoyant density in CsCl and the acid lability (9, 10). Even more, in a parallel manner to that described for FMDV, the acid sensitivity of ERAV capsid is related to the mechanism for genome release during viral entry that is triggered by the acidic pH inside cellular endosomes (5). Nevertheless, differences exist between FMDV and ERAV cell entry: ERAV uses sialic acid as a cellular receptor

Received 27 May 2016 **Accepted** 8 August 2016

Accepted manuscript posted online 17 August 2016

Citation Caridi F, Cañas-Arranz R, Vázquez-Calvo A, Sobrino F, Martín-Acebes MA. 2016. Equine rhinitis A virus mutants with altered acid resistance unveil a key role of VP3 and intrasubunit interactions in the control of the pH stability of the *Aphthovirus* capsid. J Virol 90:9725–9732. doi:10.1128/JVI.01043-16.

Editor: S. Perlman, University of Iowa

Address correspondence to Francisco Sobrino, fsobrino@cbm.csic.es.

* Present address: Angela Vázquez-Calvo, Department of Biotechnology, Instituto Nacional de Investigación y Tecnología Agraria y Alimentaria, Madrid, Spain; Miguel A. Martín-Acebes, Department of Biotechnology, Instituto Nacional de Investigación y Tecnología Agraria y Alimentaria, Madrid, Spain.

(11, 12), is more acid-resistant than FMDV, and disassembles via a transient empty particle that precedes the dissociation into pentameric subunits (4, 9). Conversely, FMDV capsid rapidly dissociates into pentameric subunits after exposure to mildly acidic pH (2, 13). The structure of both ERAV native particle and the uncoating intermediate have been resolved by X-ray crystallography providing structural information on acid-induced rearrangements of the capsid (4). Besides these data, the molecular bases that govern ERAV acid-induced dissociation and capsid stability remain poorly understood.

Deciphering the molecular basis that define capsid stability is important not only for the understanding of acid-induced uncoating but also for the improvement of aphthovirus vaccines based on empty capsids or inactivated virions (14–18). Along this line, the analysis of picornavirus mutants with altered acid sensitivities has provided valuable information to understand the mechanism of acid-dependent uncoating and to understand the molecular basis of capsid stability (13, 19–25). However, to our knowledge this kind of analysis had not been previously performed for ERAV. Having in mind all these considerations, in this work we have isolated and characterized a panel of ERAV mutants that varied on their acid resistance. The analysis of these mutants revealed parallelisms and differences between the capsid regions that govern acid-dependent disassembly and control capsid stability in ERAV and FMDV. Remarkably, VP3 appeared as a key determinant of ERAV pH stability. In addition, these mutants revealed a role of the intrasubunit interface between VP3 and VP2 or between VP3 and VP1 on acid stability. These results should be taken into account when using ERAV as surrogate of FMDV for the study of the molecular basis of the stability of the aphthovirus capsid.

MATERIALS AND METHODS

Cells and viruses. Vero cells (ATCC CCL-81) were grown on Dulbecco modified Eagle medium (DMEM; Gibco) supplemented with 5% fetal bovine serum (Gibco), 2 mM L-glutamine, and penicillin-streptomycin at 37°C in a 7% CO_2 atmosphere. ERAV was kindly provided by Carol A. Hartley (Faculty of Veterinary Sciences, The University of Melbourne). The origin of coxsackievirus B5 (CVB5) strain Faulkner has been described (26).

Infections and virus titrations. For infections in liquid medium, cell monolayers were incubated with the appropriate amount of virus diluted in DMEM without serum for 1 h at 37°C with gentle rocking every 15 min. The viral inoculum was then removed, and fresh culture medium containing 5% fetal bovine serum was added. Infected cultures were incubated at 37°C and at the desired time postinfection (p.i.), infected plates were frozen at −70°C. Virus titrations were performed by standard plaque assay in agar semisolid medium (27). To this end, 10-fold serial dilutions of the viral samples were added to Vero cell monolayers. After 1 h of incubation at 37°C, viral inoculum was removed and semisolid medium (0.5% agar, 1% fetal bovine serum, and 0.045 mg/ml DEAE-dextran in DMEM) was added. Infected plates were incubated at 37°C, and lysis plaques were visualized by staining with crystal violet 48 to 60 h p.i. The multiplicity of infection (MOI) used in each experiment was expressed as the number of PFU per cell and is indicated in the figure legends.

Acid-induced inactivation assays. A previously published protocol used for FMDV (13) was modified for ERAV. Briefly, equal amounts of viral samples (2×10^4 to 4×10^4 PFU) diluted in 50 μl of culture medium were mixed with 300 μl of phosphate-buffered saline solutions of different pHs for 30 min at room temperature, the pH was neutralized with 100 μl of 1 M Tris (pH 7.6), and the remaining infectivity in each sample was determined by titration in Vero cells as described above.

Inhibition of endosomal acidification with NH_4Cl. Vero cell monolayers were treated 1 h prior to infection with 5 or 10 mM NH_4Cl (Merck) in culture medium supplemented with 25 mM HEPES at pH 7.4 to buffer extracellular pH, and the drug was maintained throughout the rest of the infection (13).

Nucleotide sequencing. Viral RNA was extracted using TRI-Reagent (Sigma). The nucleotide sequence of the capsid coding region of ERAV was amplified by reverse transcription-PCR (RT-PCR), as reported previously (13, 28). The following forward (f) and reverse (r) synthetic oligonucleotide primer pairs were used: GGCCAAACTGTGCCTGTGAC CATG(f) and CATCTGTGTGCACGTGCATGTCCAC(r); GAGGGTTG GATCTGTGTTGA(f) and GCTTATCGGGCAGGTCAAC(r); and CGA TTAGAGTGGTGTCTGTG(f) and GCTCTCAACATCTCCAGCCA(r). Automated DNA sequencing of RT-PCR products was performed by Macrogen, Inc. (Amsterdam, The Netherlands), using the same primers. Nucleotide sequencing confirmed that the capsid coding region of the wild-type (WT) ERAV used in this study only exhibited one silent change (G222T) relative to that of the crystallized ERAV capsid (GenBank accession number FJ607143).

Molecular graphics and structure analysis. The atomic coordinates of ERAV capsid at neutral (PDB code 2WFF) and acidic pH (PDB code 2WS9) were used (4). Structures were visualized using PyMol Molecular Graphics System version 1.5.0.4 (Schrödinger, LLC). Contact information of selected residues was obtained using VIPERdb (29).

Data analysis. Data are presented as means ± standard deviations (SD). Analysis of variance (ANOVA) was performed using SPSS15 (SPSS, Inc.). Bonferroni's correction was applied for multiple comparisons. Statistically significant differences are indicated in figures by one asterisk for a P value of <0.05 or two asterisks for a P value of <0.005.

RESULTS

Isolation and characterization of NH_4Cl-resistant ERAVs. Due to its acid-triggered uncoating mechanism the infection of ERAV is impaired by drugs that inhibit endosomal acidification (5). Accordingly, we explored the possibility of isolating mutant ERAVs with increased resistance to the treatment with an inhibitor of acid-dependent uncoating. Following an approach similar to that previously used for FMDV, we selected and characterized ERAV mutants with increased resistance to the inhibition of endosomal acidification exerted by NH_4Cl (13, 22). NH_4Cl-resistant ERAVs were isolated by biological cloning in Vero cells infected with ERAV in semisolid agar medium containing 10 mM NH_4Cl. After 72 h of infection, Vero cell monolayers treated with NH_4Cl exhibited a reduction of $\sim 10^4$-fold in the number of lysis plaques produced relative to control cells, thus confirming that the drug impaired the infection of ERAV. Well isolated lysis plaques grown in the presence of NH_4Cl were picked and amplified by two serial passages in liquid medium in the presence of 10 mM NH_4Cl. Three of these amplified viral clones, termed RC3, RC8, and RC19, showed a significant increase in their resistance to treatment with 5 mM NH_4Cl compared to the parental wild-type (WT) ERAV (Fig. 1A). Thus, 5 mM NH_4Cl should raise endosomal pH to a level that is compatible with uncoating of RC3, RC8, and RC9 mutants but enough to limit the uncoating of WT virus. However, only RC3 and RC8 exhibited a significant resistance to 10 mM NH_4Cl, suggesting that the resilient phenotype of RC19 was weaker than those of RC3 and RC8. Previous studies using acid inactivation assays of FMDV have revealed that FMDV mutants resistant to NH_4Cl are more acid labile, indicating that the mechanism of escape from the inhibitory effect of this drug is based on the elevation of pH-threshold for uncoating (13, 22). When the acid sensitivity of the infectious virions was compared using an

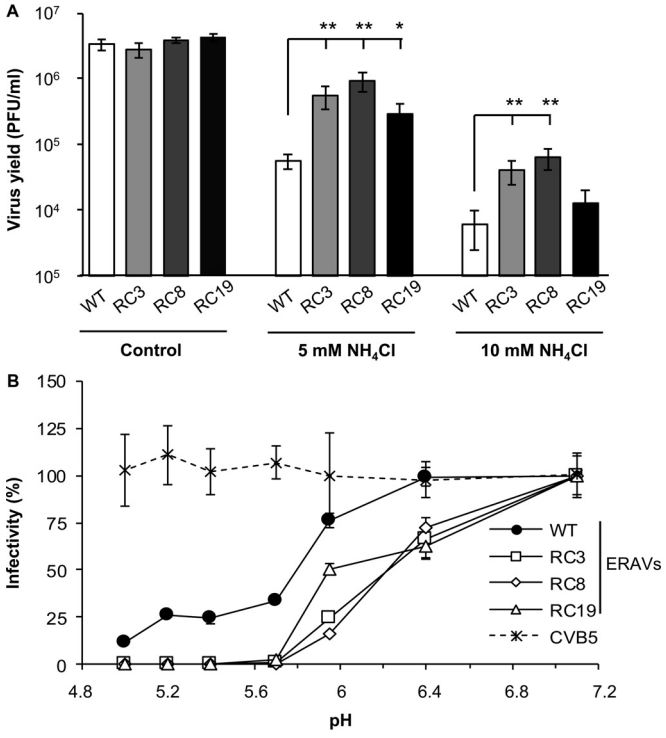

FIG 1 ERAV mutants with increased resistance to NH_4Cl display enhanced acid lability. (A) Analysis of NH_4Cl sensitivity of ERAV mutants RC3, RC8, and RC19. Monolayers of Vero cells treated or not treated with NH_4Cl were infected (MOI of 0.5 PFU/cell) with the mutants and the parental ERAV (WT). Virus yield was determined 24 h p.i. by a standard plaque assay. (B) Acid sensitivity of NH_4Cl-resistant ERAVs. Equal amounts of the different viruses were treated with acid buffers of different pHs for 30 min, neutralized, and plated. Infectivity was calculated as the percentage of PFU recovered relative to that obtained at pH 7.1. One asterisk indicates a P value of <0.05; two asterisks indicate a P value of <0.005.

acid-induced inactivation assay, the three mutants proved to be more acid sensitive than the parental WT ERAV (Fig. 1B). Interestingly, the three viruses showed similar acid inactivation profiles, although RC19 was less sensitive to acid inactivation at a pH slightly below 6. This result is consistent with the differences observed in the sensitivity to NH_4Cl treatment of these mutants, further supporting a correlation between resistance to NH_4Cl and acid sensitivity. In these experiments the enterovirus CVB5 was included as a control picornavirus with a capsid that is stable over a wide pH range (Fig. 1B). As expected, CVB5 did not show any loss of infectivity within the pH range analyzed. Overall, these results are consistent with the hypothesis that the increase in resistance to the inhibition of endosomal acidification exerted by NH_4Cl is mediated by an increase in the acid sensitivity of the virion.

Isolation and characterization of acid-resistant ERAVs. Since NH_4Cl-resistant ERAVs displayed more acid-sensitive virions than those of the WT, we decided to evaluate the opposite situation. That is, if, as reported for FMDV (23, 24), ERAV mutants with increased acid resistance displayed augmented sensitivity to NH_4Cl. Hence, as described for FMDV (24, 25, 30), ERAV mutants with increased acid resistance were isolated after serial passages preceded by acid treatment. For this purpose, 10^6 PFU of WT virus were incubated at pH 5.0 for 1 h. Then, pH was neutralized, samples were added to Vero cells, and infection was allowed to proceed in liquid medium. When cytopathic effect was observed (about 48 h p.i.) viruses were harvested. Rounds of this acid treatment/infection procedure were conducted in two independent series carried out in parallel (termed Res1 and Res2). After 10 serial passages, the acid sensitivity of the resultant populations was analyzed (Fig. 2A). Both Res1 and Res2 showed a significant increase in acid resistance (pH 5.0) compared to WT ERAV, which confirmed the selection of viruses with increased acid resistance in these populations. When the sensitivity to the inhibition of endosomal acidification using NH_4Cl was analyzed, both Res1 and Res2 displayed a significant increase in the sensitivity to NH_4Cl in comparison to WT ERAV (Fig. 2B). These results confirmed our initial hypothesis and provided additional evidence supporting the connection between stability of the capsid at acidic pH and sensitivity of ERAV to NH_4Cl.

Molecular basis for the different acid sensitivity of ERAV mutants. The complete nucleotide sequences of the capsid coding regions of acid-sensitive (NH_4Cl-resistant) mutants RC3, RC8, and RC19, as well as that of acid-resistant (NH_4Cl-sensitive) mutants Res1 and Res2 used in the experiments were determined and

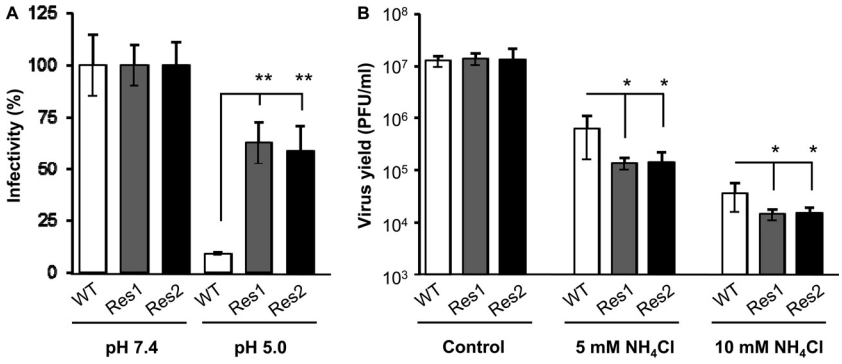

FIG 2 ERAV mutants with increased acid resistance display enhanced sensitivity to endosomal acidification blockage exerted by NH_4Cl. (A) Equal PFU amounts of the parental ERAV (WT) and the mutants Res1 and Res2 (isolated after serial passages preceded by acid treatments) were incubated with acid (pH 5.0) or neutral (pH 7.4) buffers for 30 min, neutralized, and plated on Vero monolayers. Infectivity was calculated as the percentage of PFU recovered relative to that obtained at pH 7.4. (B) Analysis of NH_4Cl sensitivity of ERAV mutants Res1 and Res2. Monolayers of Vero cells treated or not treated with NH_4Cl were infected (MOI of 0.5 PFU/cell) with the mutants and the parental ERAV, and the virus yield was determined at 24 h p.i. One asterisk indicates a P value of <0.05; two asterisks indicate a P value of <0.005.

TABLE 1 Mutations selected in the capsid coding regions of ERAV mutants with different acid sensitivities

Phenotype	Mutant	Mutation(s) selected in the capsid coding region[a]	
		Nucleotide substitution	Amino acid substitution
Acid sensitive (NH_4Cl resistant)	RC3	T1088A	VP3 F53Y
	RC8	C1537T	VP3 R203C
	RC19	A1255G	VP3 I109V
		T1758C	Synonymous
Acid resistant (NH_4Cl sensitive)	Res1	A1244G	VP3 N105S
	Res2	A1244G	VP3 N105S

[a] Numbering as for the ERAV capsid (GenBank accession number FJ607143).

compared to that of WT virus (Table 1). The viral populations RC3, RC8, and RC19 sequenced corresponded to the viral stocks produced after two serial passages in the presence of 10 mM NH_4Cl. The viral populations Res1 and Res2 sequenced were those recovered after 10 serial rounds of acid treatment and infection. Each of the five mutant ERAVs displayed a single nonsynonymous nucleotide substitution in the consensus sequence of the capsid compared to that of WT virus. Apart from the nonsynonymous replacements, mutant RC19 showed an additional silent mutation in the capsid coding region. All of the substitutions found led to nucleotide transitions, except the one found in mutant RC3 that was a transversion. Remarkably, all the amino acid replacements selected were located in VP3 protein. The nucleotide substitutions found in the three acid-sensitive mutants were different and led to amino acid replacements VP3 F53Y, R203C, and I109V in RC3, RC8, and RC19, respectively. On the other hand, the two acid-resistant viruses (Res1 and Res2) selected from two individual passage series had acquired a common nucleotide substitution that introduced amino acid replacement VP3 N105S (Table 1). The analysis of the sequence of earlier passages of Res1 and Res2 revealed that this substitution was already dominant at passages 6 and 7 for Res1 and Res2, respectively. Although the selection of the same mutation in an independent passage series could be considered surprising, there are precedents for the independent selection of common amino acid replacements increasing acid resistance of *Aphthovirus* capsid (21, 23–25). This could be the result of selective constraints that arise during the isolation of this kind of mutants that favor the selection of substitution VP3 N105S.

All the amino acid substitutions found in the acid-resistant and -sensitive mutants affected highly conserved residues in VP3 protein, which were invariant in the 25 different VP3 sequences available at GenBank from ERAV isolated in different dates and locations. Moreover, all the substitutions found in RC3, RC8, RC19, and Res2 (selected as a model for acid-resistant ERAV since Res1 and Res2 carried the same replacement) were stable after 10 serial passages in the absence of selective pressure. These amino acid substitutions were mapped on the crystal structures reported for ERAV capsid at neutral pH and for its empty particle at low pH (Fig. 3A and B). All of the replacements of acid-sensitive mutants (R203C, I109V, and F53Y) were found aligned at the intraprotomeric interface between VP2 and VP3. In addition, replacement N105S, found in acid-resistant ERAVs, was located close to these residues, at the intraprotomeric interface between VP3 and VP1. At neutral pH all of these residues appeared very close to the N terminus of VP1, which was displaced from this position at low pH (compare discontinuous circles between left and right panel in Fig. 3A and B). Moreover, all the amino acid substitutions affected residues that established interactions with other residues from VP2 and, to a lesser extent, with the N terminus of VP1 (Table 2), a capsid region involved in acid-induced rearrangements required for uncoating (4). Some of the interactions of the mutated residues were conserved at neutral and acidic pH, whereas other changed, suggesting that the four residues affected by the mutations (F53, N105, I109, and R209) were involved in acid-induced rearrangements of the viral capsid. Accordingly, the introduction of the replacements found in our mutants would probably alter this interaction pattern modulating the stability of the capsid at acidic pH. Overall, the fact that all the nonsynonymous mutations found in acid-sensitive and acid-resistant mutants were located in the coding region of VP3 indicates that this protein, and specifically its interface with VP2 and VP1, plays a pivotal role for the control of pH stability of ERAV capsid.

Fitness of ERAV mutants with altered acid sensitivity. In order to estimate the potential fitness cost derived from the mutations found in acid-sensitive and acid-resistant ERAVs, we analyzed the plaque size and the growth kinetics of the mutant virus in Vero cells. The phenotype of plaque size of all ERAV mutants was similar to that of WT virus (Fig. 4A). In addition, no major differences in the viral growth kinetics of the viruses were noticed when single-step growth curves were conducted (Fig. 4B). Taken together, these results suggested that the mutations selected in acid-sensitive and acid-resistant ERAVs did not severely affect the growth ability of the virus in cultured cells.

DISCUSSION

The capsid protects the viral genome against environmental assaults and also accomplishes vital functions, such as receptor attachment for viral entry or genome release (31). In this way, viral capsids constitute dynamic nanomachines that can undergo dramatic rearrangements during the different steps of the virus life cycle to achieve these functions (32, 33). For instance, genomic RNA must be able to leave the capsid to initiate a new round of infection, making uncoating a crucial step of the virus life cycle that provides an interesting target for antiviral design (34–39). Thus, understanding the molecular basis that govern these transitions and define capsid stability is of outstanding interest to decipher the biology of viral pathogens, as well as for the development of antiviral strategies and vaccine improvement. Considering that ERAV is becoming a model for the analysis of aphthovirus biology, we have explored the molecular basis controlling pH stability of this virus. To this end, and going one step ahead with the work made with FMDV, we have isolated and characterized a panel of ERAV mutants differing on their acid sensitivity. Overall, our results are consistent with the hypothesis that the increase in resistance to inhibition of endosomal acidification exerted by NH_4Cl is mediated by an elevation of uncoating pH. In addition, the opposite effect was observed for acid-resistant mutants, which showed an increase in the sensitivity to inhibition of endosomal acidification exerted by NH_4Cl. These results provided further functional evidence of the link between uncoating mechanism and acidic pH inside cellular endosomes (5). The ERAV mutants with altered pH stability that we isolated showed plaque sizes

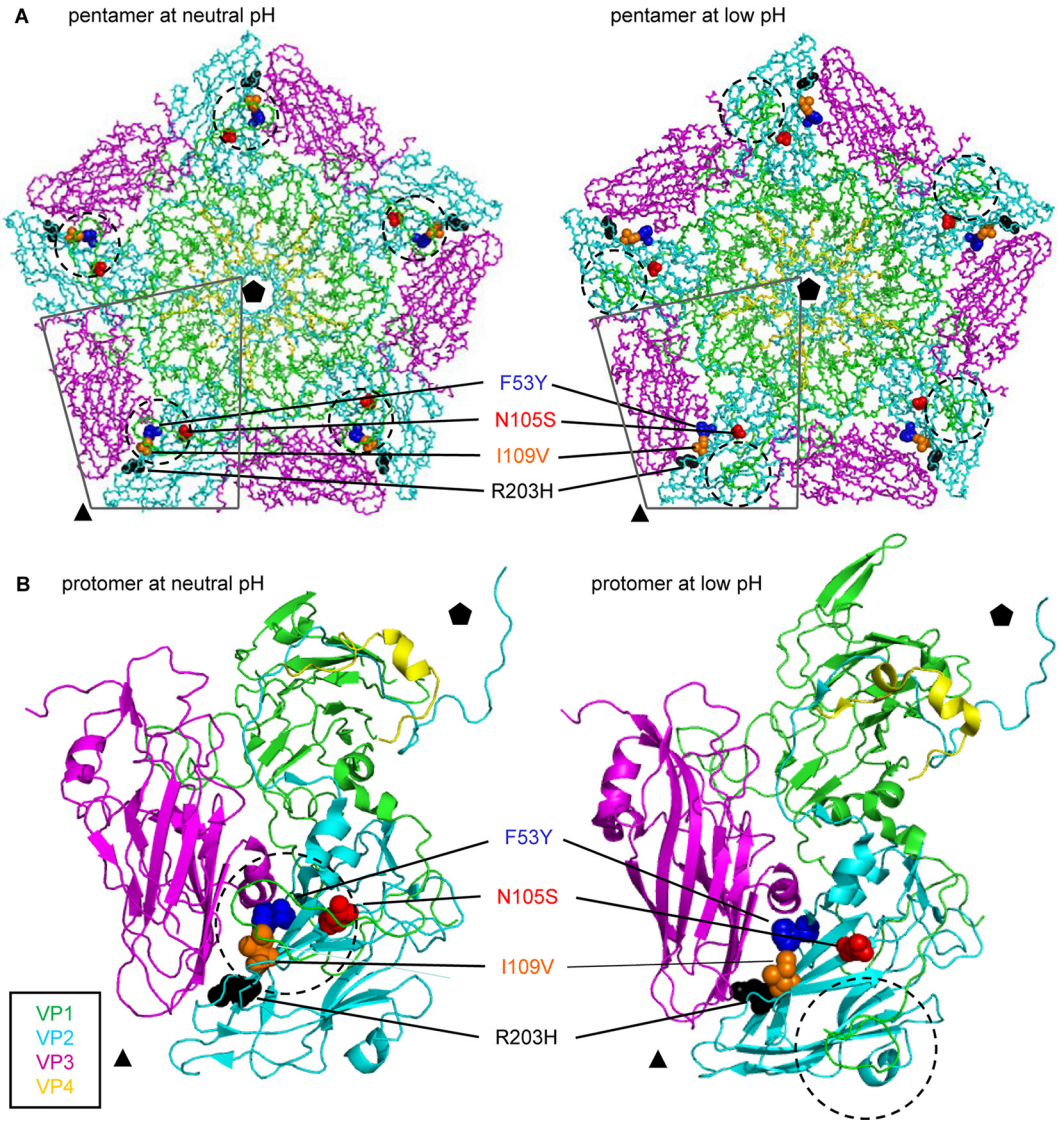

FIG 3 Location of mutations affecting acid stability of ERAV. (A) Inside schematic view of a pentameric subunit in the capsid of ERAV at neutral (left panel) or acid pH (right panel) displaying the location of amino acid residues found to be substituted in mutants (spheres). The position of a single protomer is indicated by gray lines. Discontinuous circles indicate the location of the N terminus of VP1. Only amino acid main chains are shown for clarity. The atomic coordinates of ERAV capsid at neutral (PDB code 2WFF) and acidic pH (PDB code 2WS9) were used (4). (B) Cartoon representation of the protomer highlighted in panel A showing the position of the amino acid replacements found in ERAV mutants at neutral (left) or low (right) pH. Circles indicate the location of the N terminus of VP1. The positions of 5- and 3-fold symmetry axes are denoted by pentagons and triangles, respectively. VP1 is green, VP2 is magenta, VP3 is cyan, and VP4 is yellow.

TABLE 2 Contacts established by capsid residues mutated in ERAVs with altered pH stability

	Capsid residues establishing contact with the VP3 residue[a]	
VP3 residue	Neutral pH	Low pH
F53	VP2 **Y152**, S156, L199	VP2 S156, **L162,** L199
N105	**VP1 T13**	
I109	VP2 L162, N164 **VP1 G5**	VP2 L162, N164
R209	VP2 **S121**, S200, E201, T203	VP2 S200, E201, T203

[a] Contact information was retrieved from VIPERdb (29). Contacts that vary between neutral- and low-pH structures are indicated in boldface.

and growth kinetics similar to those of the WT virus, suggesting that, as in the case of FMDV, the selection of viruses with altered acid stability, including those that were acid resistant, can be performed with a low fitness cost *in vitro* (13, 21–25). This is supported by the stability of these amino acid substitutions noticed after 10 serial passages of the mutants in the absence of selective pressure. Nevertheless, it cannot be excluded that these replacements could lead to detrimental effects *in vivo*, as described for FMDV (40). In fact, it is conceivable that WT ERAV has evolved an optimal pH for uncoating and that displacement of this value could result in attenuation *in vivo*.

Interestingly, all the amino acid replacements found in ERAV

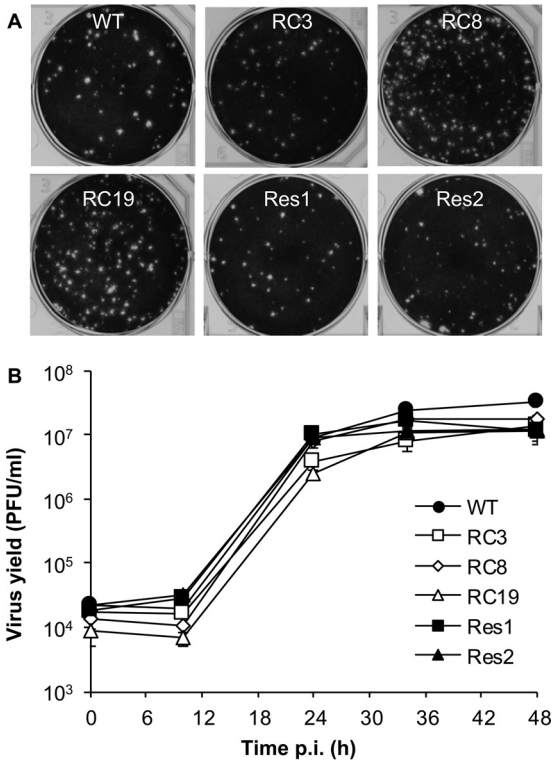

FIG 4 Fitness analysis of ERAV mutants with altered acid sensitivity. (A) Lysis plaques of the parental ERAV (WT), acid-sensitive ERAV mutants (RC3, RC8, and RC19) and acid-resistant ERAV mutants (Res1 and Res2). Vero cells were infected in semisolid agar medium, and plaques were visualized by staining with crystal violet at 60 h p.i. (B) Single-step growth curve analysis of ERAVs indicated in panel A. Vero cells were infected (MOI of 1 PFU/cell), and the virus titers in the supernatants were determined by plaque assay at different times postinfection.

mutants with different acid stability were mapped in VP3. The detailed examination of the mutated residues indicated did not reveal a common side chain substitution pattern. Acid-sensitive mutants RC3 and RC19 introduced amino acid replacements that preserved hydrophobicity (F53Y and I109V), in one case displaying a bulkier residue with the introduction of a hydroxyl group (F53Y) and in the other case a smaller one (I109V). On the other hand, the acid-sensitive mutant RC8 displayed a loss of positive charge and the introduction of a smaller residue (R203C). Interestingly, substitution R209C abolished a positive charge that interacted with the negatively charged VP2 E201, suggesting that the loss of the electrostatic charge of this residue mediates the mechanism of action of this mutant. In the case of the acid-resistant viruses Res1 and Res2, the replacement selected maintains a polar residue but with a smaller side chain (N105S). N105, I109, and R203 were located in β-strands of the capsid that were found at both neutral and acidic pH (4). In FMDV, mutations also affecting the pH stability of the capsid at residues VP3 116, 118, and 123 have been located within another β-strand of VP3 (13, 22), although these residues were located close to the interpentameric interface, not at the intraprotomeric interface between VP3 and VP2 as occurred in ERAV. In this way, ERAV mutants VP3 F53Y, I109V, and R203C demonstrate for the first time that the interface between VP3 and VP2 within the same protomer constitutes a key capsid region controlling pH stability. All of these residues also map close to the N terminus of VP1 in the native ERAV particle. Even more, replacement VP3 N105S is located at the interface between VP3 and the N terminus of VP1, and replacement VP3 I109V also affected an amino acid interacting with the N terminus of VP1 at neutral pH. Both interactions are lost in the empty particle as a results of exposure to acidic pH. This is consistent with structural data supporting that the N terminus of VP1 is key for aphthovirus uncoating and undergoes a profound rearrangement during the transition between the virion to the low-pH empty particle uncoating intermediate (4). Thus, these data further support the importance of the N terminus of VP1 in regulating the pH stability of aphthovirus capsid, as previously documented for FMDV by the selection of amino acid replacements in the N terminus of FMDV VP1 (22–25). Remarkably, the involvement of the N terminus of VP1 in uncoating is a conserved feature within the *Picornaviridae* family (41–43). The relevance of the intraprotomeric interface between VP3 and VP2 on aphthovirus pH stability had not been previously assessed, since FMDV pH stability was mainly associated with the N terminus of VP1 and the residues located at the pentameric interface (13, 21–25, 44–46). However, independent studies have shown that acid resistant FMDVs from different serotypes display a common amino acid substitution (VP2 H145Y) in a residue located close to the center of the protomer and the interface between VP3 and VP2 and that interacted with the N terminus of VP1 (21, 24). All of these data are consistent with the involvement of the contacts among VP3, VP2, and VP1 in the central region of the protomer in the regulation of aphthovirus acid stability. Considering the importance for capsid stability of the intersubunit interactions (either interprotomeric or interpentameric) documented for FMDV (14, 47), the identification in this study of the intraprotomeric interface as an important regulator of ERAV capsid expands the regions that govern aphthovirus capsid stability.

As commented above, all of the replacements found in ERAV mutants were located in VP3, which is the most conserved of the structural proteins between ERAV and FMDV (4). However, the different locations of pH-altering mutations in FMDV and ERAV capsids could reflect differences between FMDV and ERAV uncoating. In fact, ERAV uncoating is produced by a stable transient empty particle intermediate, while the experimental evidence for this intermediate is scarce in the case of FMDV (48). Hence, the current model for FMDV uncoating supports its rapid dissociation into pentameric subunits after exposure to mildly acidic pH (13, 49). The parallelism between pH mutants of ERAV and FMDV (the involvement of VP3 and connections with the VP1 N terminus) is consistent with the hypothesis of a common ancestral mechanism for aphthovirus uncoating (4), but the differences in the location of the mutations support the specialization and diversification of ERAV and FMDV uncoating mechanisms as a product of viral evolution.

In summary, we provide novel evidence that VP3 and especially the intrasubunit region that forms the interface among VP3, VP2, and VP1 within the same protomer, is a key regulator of the pH stability of ERAV capsid. These results expand our knowledge of the regions involved in the regulation of aphthovirus capsid stability and could contribute to the improvement of vaccine strategies based on capsid stabilization that are currently being addressed.

ACKNOWLEDGMENTS

We thank Carol A. Hartley for the ERAV isolate and N. Verdaguer for critical readings of the manuscript.

This study was supported by Spanish grants BIO2011-24351, AGL2014-52395-C2-01, and S2013/ABI-2906-PLATESA (Comunidad Autónoma de Madrid) (to F.S.), and AGL2014-56518-JIN (to M.A.M.-A.). Work at the Centro de Biología Molecular Severo Ochoa was also supported by Fundación Ramón Areces. The funders had no role in study design, data collection and interpretation, or the decision to submit the work for publication.

FUNDING INFORMATION

This work, including the efforts of Francisco Sobrino, was funded by Comunidad Autonoma de Madrid (S2013/ABI-2906-PLATESA). This work, including the efforts of Francisco Sobrino, was funded by Ministerio de Economia y Competitividad (MINECO) (BIO2011-24351 and AGL2014-52395-C2-01). This work, including the efforts of Miguel Angel Martin-Acebes, was funded by Ministerio de Economia y Competitividad (MINECO) (AGL2014-56518-JIN).

The funders had no role in study design, data collection and interpretation, or the decision to submit the work for publication.

REFERENCES

1. **Horsington J, Lynch SE, Gilkerson JR, Studdert MJ, Hartley CA.** 2013. Equine picornaviruses: well known but poorly understood. Vet Microbiol **167:**78–85. http://dx.doi.org/10.1016/j.vetmic.2013.05.012.
2. **Diaz-Mendez A, Hewson J, Shewen P, Nagy E, Viel L.** 2014. Characteristics of respiratory tract disease in horses inoculated with equine rhinitis A virus. Am J Vet Res **75:**169–178. http://dx.doi.org/10.2460/ajvr.75.2.169.
3. **Li F, Browning GF, Studdert MJ, Crabb BS.** 1996. Equine rhinovirus 1 is more closely related to foot-and-mouth disease virus than to other picornaviruses. Proc Natl Acad Sci U S A **93:**990–995. http://dx.doi.org/10.1073/pnas.93.3.990.
4. **Tuthill TJ, Harlos K, Walter TS, Knowles NJ, Groppelli E, Rowlands DJ, Stuart DI, Fry EE.** 2009. Equine rhinitis A virus and its low pH empty particle: clues towards an aphthovirus entry mechanism? PLoS Pathog **5:**e1000620. http://dx.doi.org/10.1371/journal.ppat.1000620.
5. **Groppelli E, Tuthill TJ, Rowlands DJ.** 2010. Cell entry of the aphthovirus equine rhinitis A virus is dependent on endosome acidification. J Virol **84:**6235–6240. http://dx.doi.org/10.1128/JVI.02375-09.
6. **Osiceanu AM, Murao LE, Kollanur D, Swinnen J, De Vleeschauwer AR, Lefebvre DJ, De Clercq K, Neyts J, Goris N.** 2014. In vitro surrogate models to aid in the development of antivirals for the containment of foot-and-mouth disease outbreaks. Antiviral Res **105:**59–63. http://dx.doi.org/10.1016/j.antiviral.2014.02.009.
7. **Bakker SE, Groppelli E, Pearson AR, Stockley PG, Rowlands DJ, Ranson NA.** 2014. Limits of structural plasticity in a picornavirus capsid revealed by a massively expanded equine rhinitis A virus particle. J Virol **88:**6093–6099. http://dx.doi.org/10.1128/JVI.01979-13.
8. **Rueckert RR.** 1996. *Picornaviridae*: the viruses and their replication, p 609–654. *In* Fields B, Knipe DM, Howley PM (ed), Virology. Lippincott-Raven Publishers, Philadelphia, PA.
9. **Newman JF, Rowlands DJ, Brown F.** 1973. A physicochemical subgrouping of the mammalian picornaviruses. J Gen Virol **18:**171–180. http://dx.doi.org/10.1099/0022-1317-18-2-171.
10. **Newman JF, Rowlands DJ, Brown F, Goodridge D, Burrows R, Steck F.** 1977. Physicochemical characterization of two serologically unrelated equine rhinoviruses. Intervirology **8:**145–154. http://dx.doi.org/10.1159/000148889.
11. **Stevenson RA, Huang JA, Studdert MJ, Hartley CA.** 2004. Sialic acid acts as a receptor for equine rhinitis A virus binding and infection. J Gen Virol **85:**2535–2543. http://dx.doi.org/10.1099/vir.0.80207-0.
12. **Fry EE, Tuthill TJ, Harlos K, Walter TS, Rowlands DJ, Stuart DI.** 2010. Crystal structure of equine rhinitis A virus in complex with its sialic acid receptor. J Gen Virol **91:**1971–1977. http://dx.doi.org/10.1099/vir.0.020420-0.
13. **Martin-Acebes MA, Rincon V, Armas-Portela R, Mateu MG, Sobrino F.** 2010. A single amino acid substitution in the capsid of foot-and-mouth disease virus can increase acid lability and confer resistance to acid-dependent uncoating inhibition. J Virol **84:**2902–2912. http://dx.doi.org/10.1128/JVI.02311-09.
14. **Mateo R, Diaz A, Baranowski E, Mateu MG.** 2003. Complete alanine scanning of intersubunit interfaces in a foot-and-mouth disease virus capsid reveals critical contributions of many side chains to particle stability and viral function. J Biol Chem **278:**41019–41027. http://dx.doi.org/10.1074/jbc.M304990200.
15. **Mateo R, Luna E, Rincon V, Mateu MG.** 2008. Engineering viable foot-and-mouth disease viruses with increased thermostability as a step in the development of improved vaccines. J Virol **82:**12232–12240. http://dx.doi.org/10.1128/JVI.01553-08.
16. **Porta C, Kotecha A, Burman A, Jackson T, Ren J, Loureiro S, Jones IM, Fry EE, Stuart DI, Charleston B.** 2013. Rational engineering of recombinant picornavirus capsids to produce safe, protective vaccine antigen. PLoS Pathog **9:**e1003255. http://dx.doi.org/10.1371/journal.ppat.1003255.
17. **Rincon V, Rodriguez-Huete A, Lopez-Arguello S, Ibarra-Molero B, Sanchez-Ruiz JM, Harmsen MM, Mateu MG.** 2014. Identification of the structural basis of thermal lability of a virus provides a rationale for improved vaccines. Structure **22:**1560–1570. http://dx.doi.org/10.1016/j.str.2014.08.019.
18. **Kotecha A, Seago J, Scott K, Burman A, Loureiro S, Ren J, Porta C, Ginn HM, Jackson T, Perez-Martin E, Siebert CA, Paul G, Huiskonen JT, Jones IM, Esnouf RM, Fry EE, Maree FF, Charleston B, Stuart DI.** 2015. Structure-based energetics of protein interfaces guides foot-and-mouth disease virus vaccine design. Nat Struct Mol Biol **22:**788–794. http://dx.doi.org/10.1038/nsmb.3096.
19. **Skern T, Torgersen H, Auer H, Kuechler E, Blaas D.** 1991. Human rhinovirus mutants resistant to low pH. Virology **183:**757–763. http://dx.doi.org/10.1016/0042-6822(91)91006-3.
20. **Giranda VL, Heinz BA, Oliveira MA, Minor I, Kim KH, Kolatkar PR, Rossmann MG, Rueckert RR.** 1992. Acid-induced structural changes in human rhinovirus 14: possible role in uncoating. Proc Natl Acad Sci U S A **89:**10213–10217. http://dx.doi.org/10.1073/pnas.89.21.10213.
21. **Vazquez-Calvo A, Caridi F, Sobrino F, Martin-Acebes MA.** 2014. An increase in acid resistance of foot-and-mouth disease virus capsid is mediated by a tyrosine replacement of the VP2 histidine previously associated with VP0 cleavage. J Virol **88:**3039–3042. http://dx.doi.org/10.1128/JVI.03222-13.
22. **Caridi F, Vazquez-Calvo A, Sobrino F, Martin-Acebes MA.** 2015. The pH stability of foot-and-mouth disease virus particles is modulated by residues located at the pentameric interface and in the N terminus of VP1. J Virol **89:**5633–5642. http://dx.doi.org/10.1128/JVI.03358-14.
23. **Martin-Acebes MA, Vazquez-Calvo A, Rincon V, Mateu MG, Sobrino F.** 2011. A single amino acid substitution in the capsid of foot-and-mouth disease virus can increase acid resistance. J Virol **85:**2733–2740. http://dx.doi.org/10.1128/JVI.02245-10.
24. **Wang H, Song S, Zeng J, Zhou G, Yang D, Liang T, Yu L.** 2014. Single amino acid substitution of VP1 N17D or VP2 H145Y confers acid-resistant phenotype of type Asia1 foot-and-mouth disease virus. Virol Sin **29:**103–111. http://dx.doi.org/10.1007/s12250-014-3426-x.
25. **Liang T, Yang D, Liu M, Sun C, Wang F, Wang J, Wang H, Song S, Zhou G, Yu L.** 2014. Selection and characterization of an acid-resistant mutant of serotype O foot-and-mouth disease virus. Arch Virol **159:**657–667. http://dx.doi.org/10.1007/s00705-013-1872-7.
26. **Martin-Acebes MA, Blazquez AB, Jimenez de Oya N, Escribano-Romero E, Saiz JC.** 2011. West Nile virus replication requires fatty acid synthesis but is independent on phosphatidylinositol-4-phosphate lipids. PLoS One **6:**e24970. http://dx.doi.org/10.1371/journal.pone.0024970.
27. **Martin-Acebes MA, Gonzalez-Magaldi M, Sandvig K, Sobrino F, Armas-Portela R.** 2007. Productive entry of type C foot-and-mouth disease virus into susceptible cultured cells requires clathrin and is dependent on the presence of plasma membrane cholesterol. Virology **369:**105–118. http://dx.doi.org/10.1016/j.virol.2007.07.021.
28. **Vazquez-Calvo A, Saiz JC, Sobrino F, Martin-Acebes MA.** 2016. First complete coding sequence of a Spanish isolate of swine vesicular disease virus. Genome Announc **4:**e01742-15. http://dx.doi.org/10.1128/genomeA.01742-15.
29. **Carrillo-Tripp M, Shepherd CM, Borelli IA, Venkataraman S, Lander G, Natarajan P, Johnson JE, Brooks CL, III, Reddy VS.** 2009. VIPERdb2: an enhanced and web API enabled relational database for structural virology. Nucleic Acids Res **37:**D436–D442. http://dx.doi.org/10.1093/nar/gkn840.

30. **Twomey T, France LL, Hassard S, Burrage TG, Newman JF, Brown F.** 1995. Characterization of an acid-resistant mutant of foot-and-mouth disease virus. Virology **206:**69–75. http://dx.doi.org/10.1016/S0042-6822(95)80020-4.
31. **Mateu MG.** 2013. Assembly, stability, and dynamics of virus capsids. Arch Biochem Biophys **531:**65–79. http://dx.doi.org/10.1016/j.abb.2012.10.015.
32. **Johnson JE.** 2010. Virus particle maturation: insights into elegantly programmed nanomachines. Curr Opin Struct Biol **20:**210–216. http://dx.doi.org/10.1016/j.sbi.2010.01.004.
33. **Koudelka KJ, Pitek AS, Manchester M, Steinmetz NF.** 2015. Virus-based nanoparticles as versatile nanomachines Annu Rev Virol **2:**22.
34. **De Colibus L, Wang X, Spyrou JA, Kelly J, Ren J, Grimes J, Puerstinger G, Stonehouse N, Walter TS, Hu Z, Wang J, Li X, Peng W, Rowlands DJ, Fry EE, Rao Z, Stuart DI.** 2014. More-powerful virus inhibitors from structure-based analysis of HEV71 capsid-binding molecules. Nat Struct Mol Biol **21:**282–288. http://dx.doi.org/10.1038/nsmb.2769.
35. **Smith TJ, Kremer MJ, Luo M, Vriend G, Arnold E, Kamer G, Rossmann MG, McKinlay MA, Diana GD, Otto MJ.** 1986. The site of attachment in human rhinovirus 14 for antiviral agents that inhibit uncoating. Science **233:**1286–1293. http://dx.doi.org/10.1126/science.3018924.
36. **Fox MP, Otto MJ, McKinlay MA.** 1986. Prevention of rhinovirus and poliovirus uncoating by WIN 51711, a new antiviral drug. Antimicrob Agents Chemother **30:**110–116. http://dx.doi.org/10.1128/AAC.30.1.110.
37. **Rosenwirth B, Oren DA, Arnold E, Kis ZL, Eggers HJ.** 1995. SDZ 35-682, a new picornavirus capsid-binding agent with potent antiviral activity. Antiviral Res **26:**65–82. http://dx.doi.org/10.1016/0166-3542(94)00066-H.
38. **Liu Y, Sheng J, Fokine A, Meng G, Shin WH, Long F, Kuhn RJ, Kihara D, Rossmann MG.** 2015. Structure and inhibition of EV-D68, a virus that causes respiratory illness in children. Science **347:**71–74. http://dx.doi.org/10.1126/science.1261962.
39. **Lacroix C, Querol-Audi J, Roche M, Franco D, Froeyen M, Guerra P, Terme T, Vanelle P, Verdaguer N, Neyts J, Leyssen P.** 2014. A novel benzonitrile analogue inhibits rhinovirus replication. J Antimicrob Chemother **69:**2723–2732. http://dx.doi.org/10.1093/jac/dku200.
40. **Vazquez-Calvo A, Caridi F, Rodriguez-Pulido M, Borrego B, Saiz M, Sobrino F, Martin-Acebes MA.** 2012. Modulation of foot-and-mouth disease virus pH threshold for uncoating correlates with differential sensitivity to inhibition of cellular Rab GTPases and decreases infectivity in vivo. J Gen Virol **93:**2382–2386. http://dx.doi.org/10.1099/vir.0.045419-0.
41. **Pickl-Herk A, Luque D, Vives-Adrian L, Querol-Audi J, Garriga D, Trus BL, Verdaguer N, Blaas D, Caston JR.** 2013. Uncoating of common cold virus is preceded by RNA switching as determined by X-ray and cryo-EM analyses of the subviral A-particle. Proc Natl Acad Sci U S A **110:**20063–20068. http://dx.doi.org/10.1073/pnas.1312128110.
42. **Lyu K, Ding J, Han JF, Zhang Y, Wu XY, He YL, Qin CF, Chen R.** 2014. Human enterovirus 71 uncoating captured at atomic resolution. J Virol **88:**3114–3126. http://dx.doi.org/10.1128/JVI.03029-13.
43. **Ren J, Wang X, Hu Z, Gao Q, Sun Y, Li X, Porta C, Walter TS, Gilbert RJ, Zhao Y, Axford D, Williams M, McAuley K, Rowlands DJ, Yin W, Wang J, Stuart DI, Rao Z, Fry EE.** 2013. Picornavirus uncoating intermediate captured in atomic detail. Nat Commun **4:**1929. http://dx.doi.org/10.1038/ncomms2889.
44. **Biswal JK, Das B, Sharma GK, Khulape SA, Pattnaik B.** 2012. Role of a single amino acid substitution of VP3 H142D for increased acid resistance of foot-and-mouth disease virus serotype A. Virus Genes **52:**235–243. http://dx.doi.org/10.1007/s11262-016-1294-1.
45. **Maree FF, Blignaut B, de Beer TA, Rieder E.** 2013. Analysis of SAT type foot-and-mouth disease virus capsid proteins and the identification of putative amino acid residues affecting virus stability. PLoS One **8:**e61612. http://dx.doi.org/10.1371/journal.pone.0061612.
46. **Ellard FM, Drew J, Blakemore WE, Stuart DI, King AM.** 1999. Evidence for the role of His-142 of protein 1C in the acid-induced disassembly of foot-and-mouth disease virus capsids. J Gen Virol **80**(Part 8)**:**1911–1918. http://dx.doi.org/10.1099/0022-1317-80-8-1911.
47. **Rincon V, Rodriguez-Huete A, Mateu MG.** 2015. Different functional sensitivity to mutation at intersubunit interfaces involved in consecutive stages of foot-and-mouth disease virus assembly. J Gen Virol **96:**2595–2606. http://dx.doi.org/10.1099/vir.0.000187.
48. **Rowlands DJ, Sangar DV, Brown F.** 1975. A comparative chemical and serological study of the full and empty particles of foot-and mouth disease virus. J Gen Virol **26:**227–238. http://dx.doi.org/10.1099/0022-1317-26-3-227.
49. **Baxt B, Bachrach HL.** 1980. Early interactions of foot-and-mouth disease virus with cultured cells. Virology **104:**42–55. http://dx.doi.org/10.1016/0042-6822(80)90364-5.